Structural and Kinetic Characterization of an Acyl Transferase Ribozyme

Hiroaki Suga,[†] Peter A. Lohse,[‡] and Jack W. Szostak*

Contribution from the Department of Molecular Biology, Massachusetts General Hospital, Boston, Massachusetts 02114

Received July 21, 1997

Abstract: We have previously isolated, by in vitro selection, an acyl-transferase ribozyme that is capable of transferring a biotinylated methionyl group from the 3′ end of a hexanucleotide substrate to its own 5′-hydroxyl. Comparison of the sequences of a family of evolved derivatives of this ribozyme allowed us to generate a model of the secondary structure of the ribozyme. The predicted secondary structure was extensively tested and confirmed by single-mutant and compensatory double-mutant analyses. The role of the template domain in aligning the acyl-donor oligonucleotide and acyl-acceptor region of the ribozyme was confirmed in a similar manner. The significance of different domains of the ribozyme structure and the importance of two tandem G:U wobble base pairs in the template domain were studied by kinetic characterization of mutant ribozymes. The wobble base pairs contribute to the catalytic rate enhancement, but only in the context of the complete ribozyme; the ribozyme in turn alters the metal binding properties of this site. Competitive inhibition experiments with unacylated substrate oligonucleotide are consistent with the ribozyme acting to stabilize substrate binding to the template, while negative interactions with the aminoacyl portion of the substrate destabilize binding.

Introduction

In vitro selection and evolution are useful techniques for isolating nucleic acid molecules with novel activities.[1−4] We and others have used this technique to isolate catalytically active RNAs (ribozymes)[5−13] and DNAs (deoxyribozymes)[14−17] from pools of random nucleic acid sequences. We have recently isolated a ribozyme with acyl-transferase activity[18] that is able to transfer a biotinylated methionyl (Biotin-Met) group from the 3′ end of a substrate hexanucleotide to a hydroxyl or amino group at its own 5′ end (Figure 1). This ribozyme was isolated following four rounds of selection from a pool of random sequences, followed by three rounds of continued selection with mutagenic amplification and an additional four rounds of increasingly stringent selection. Approximately 90% of the sequenced clones derived from the eleventh round of the acyl-transferase selection fell into one class with about 90% identity (Figure 2A).[18] Most of the divergence from the common ancestor of these sequences presumably occurred during the course of the mutagenic PCR[19,20] in rounds 5−7 of the selection. An invariant region of these sequences, located near the 3′ end, is complementary to both the hexanucleotide substrate and to the constant 5′ end of the ribozyme (Figure 2). This domain is thought to act as a template to bring the biotinylated methionyl group, attached to the 3′ end of the hexanucleotide, into close proximity with the hydroxyl group at the 5′ end of the ribozyme.

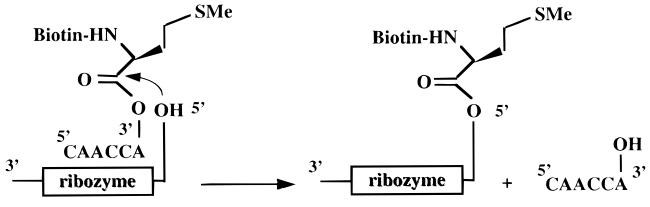

Figure 1. Schematic representation of acyl transfer reaction catalyzed by ribozyme.

The acyl-transferase ribozyme has been extensively characterized with respect to the role of metal ions in its catalytic activity.[21] The catalytic activity of the ribozyme is dependent upon divalent metal ions, but this activity does not follow the pK_a rule for metal ion bound water, suggesting that, unlike most ribozymes, such as the hammerhead and RNase P, the role of the metal ion is not simply to facilitate deprotonation of the attacking nucleophile. Furthermore, cobalt(III) hexaammine, $Co(NH_3)_6^{3+}$, an exchange-inert metal ion, supports acyl-transfer activity, showing that the metal ion interacts with the substrate and ribozyme via outer-sphere coordination. The ribozyme must

[†] Current address: Department of Chemistry, State University of New York at Buffalo, 657 Natural Sciences Complex, Buffalo, NY 14260-3000.
[‡] Current address: Phylos Inc., 300 Putnam St., Cambridge, MA 02138.

(1) Hager, A. J.; Pollard, J. D.; Szostak, J. W. *Chem. Biol.* **1996**, *3*, 717−725.
(2) Lorsch, J. R.; Szostak, J. W. *Acc. Chem. Res* **1996**, *29*, 103−110.
(3) Breaker, R. R.; Joyce, G. F. *Trands Biotechnol.* **1994**, *12*, 268−275.
(4) Gold, L.; Polisky, B.; Uhlenbeck, O. C.; Yarus, M. *Annu. Rev. Biochem.* **1995**, *64*, 763−797.
(5) Bartel, D. P.; Szostak, J. W. *Science* **1993**, *261*, 1411−1418.
(6) Lorsch, J. R.; Szostak, J. W. *Nature* **1994**, *371*, 31−36.
(7) Ekland, E. H.; Szostak, J. W.; Bartel, D. P. *Science* **1995**, *269*, 364−370.
(8) Ekland, E. H.; Bartel, D. P. *Nature* **1996**, *382*, 373−376.
(9) Wilson, C.; Szostak, J. W. *Nature* **1995**, *374*, 777−782.
(10) Prudent, J. R.; Uno, T.; Schultz, P. G. *Science* **1994**, *264*, 1924−1927.
(11) Illangasekare, M.; Sanchez, G.; Nickles, T.; Yarus, M. *Science* **1995**, *267*, 643−647.
(12) Wright, M. C.; Joyce, G. F. *Science* **1997**, *256*, 614−617.
(13) Pan, T.; Uhlenbeck, O. C. *Biochemistry* **1992**, *31*, 3887−3895.
(14) Cuenoud, B.; Szostak, J. W. *Nature* **1995**, *375*, 611−614.
(15) Breaker, R. R.; Joyce, G. F. *Chem. Biol.* **1994**, *1*, 223−339.
(16) Breaker, R. R.; Joyce, G. F. *Chem. Biol.* **1995**, *2*, 655−660.
(17) Wechker, M.; Smith, D.; Gold, L. *RNA* **1996**, *2*, 982−994.
(18) Lohse, P. A.; Szostak, J. W. *Nature* **1996**, *381*, 442−444.
(19) Joyce, G. F. *Gene* **1989**, *82*, 83−87.
(20) Beaudry, A. A.; Joyce, G. F. *Science* **1992**, *257*, 635−641.
(21) Suga, H.; Cowan, J. A.; Szostak, J. W. Submitted for publication.

S0002-7863(97)02472-4 CCC: $15.00
Published on Web 01/30/1998

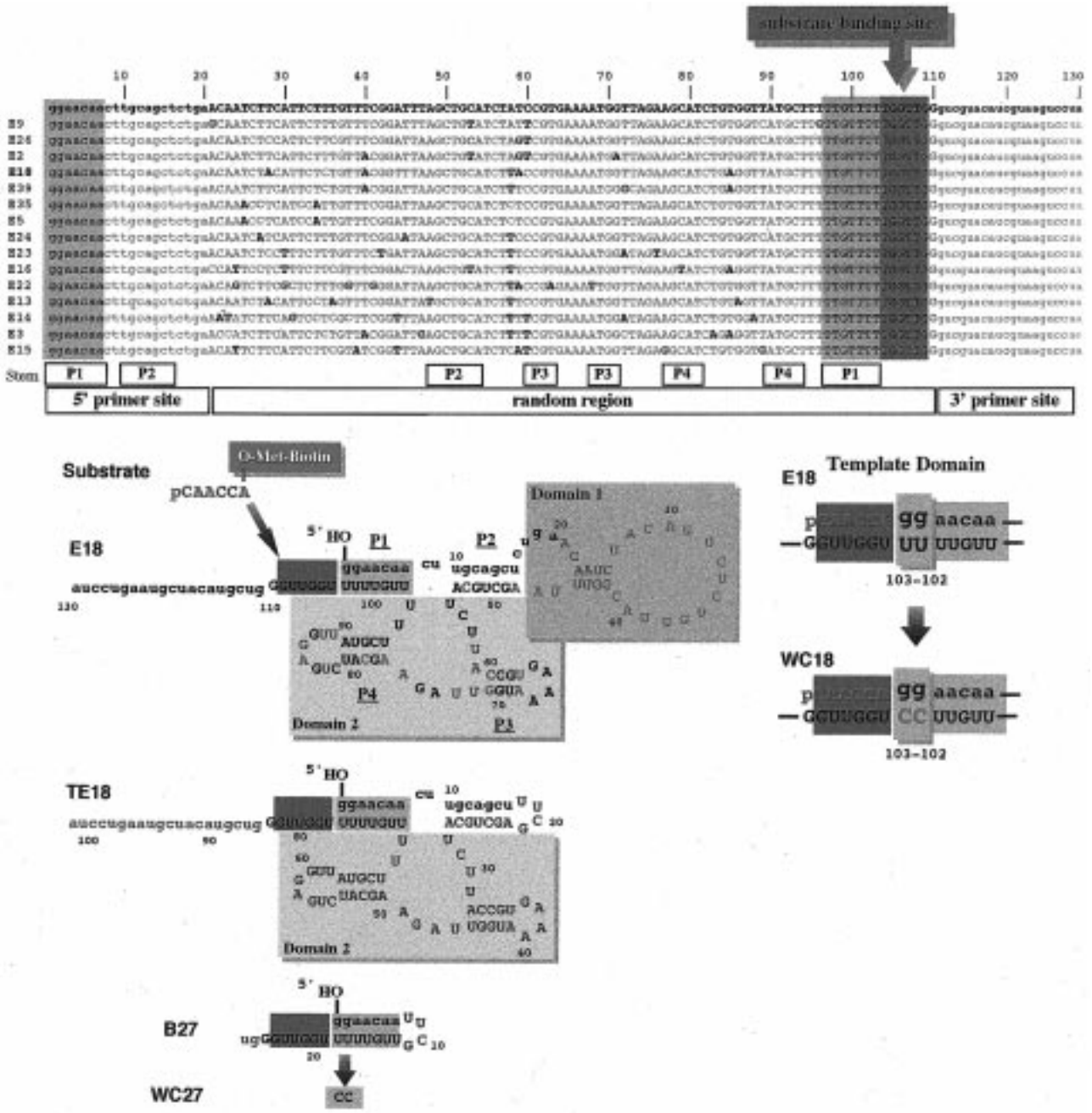

Figure 2. (A) Sequence alignment of the class 1 acyl transferases. The primer sequences and the sequences in the random region are in lower and upper cases, respectively. Deviations of individual clones from the consensus sequence (top line) are highlighted in colored letters (G in red, to C in orange, to T in green, to A in blue). (B) Secondary structures of acyl-transferase ribozymes: (left) The wild-type ribozyme E18, the deletion derivative TE18, and the isolated template domains are shown. Green boxes indicate the substrate binding site for each ribozyme. The absolutely conserved bases found in E18 are shown in bold upper case. (right) The template domain of E18, showing the mutations of tandem wobble base pairs to Watson−Crick base pairs in WC18, highlighted in red letters.

therefore normally use the hydrated form of Mg^{2+}, $Mg(H_2O)_6^{2+}$, for catalysis. It is likely that only a single metal ion is involved in the acyl-transfer reaction catalyzed by the ribozyme and that the binding site for this catalytic metal ion is comprised, at least in part, of a pair of tandem wobble base pairs located adjacent to the site of the reaction in the template domain.

Secondary Structure of Wild-Type Ribozyme. A secondary structure model for the nontemplate part of the ribozyme was predicted by the GCG MulFold program (Figure 2B), using the sequence of the E18 clone. The predicted secondary structure contains three stems (paired regions P2, P3, and P4) outside of the template region (P1) that are well conserved in the set of class 1 sequences. The existence of these paired regions is supported in some cases by the occurrence of covarying mutations that change one potential Watson−Crick base pair to a different base pair or, more commonly, by the preferential occurrence of single mutations that change a Watson−Crick base pair to a wobble base pair. For example, the sequences that make up stem P2 are largely conserved, except for a C53U mutation which converts the G11:C53 base pair to a wobble base pair (clones E2, E9, and E16). In stem P3, the potential Watson−Crick base pair C60:G71 mutated to a wobble base pair U60:G71 (clones E3, E9, E14, E15, and E26) or changed to a different Watson−Crick base pair, U60:A71, in clone E2. Also in stem P3, U63:A68 changed to A63:U68 in clone E22. In stem P4, two Watson Crick to G:U

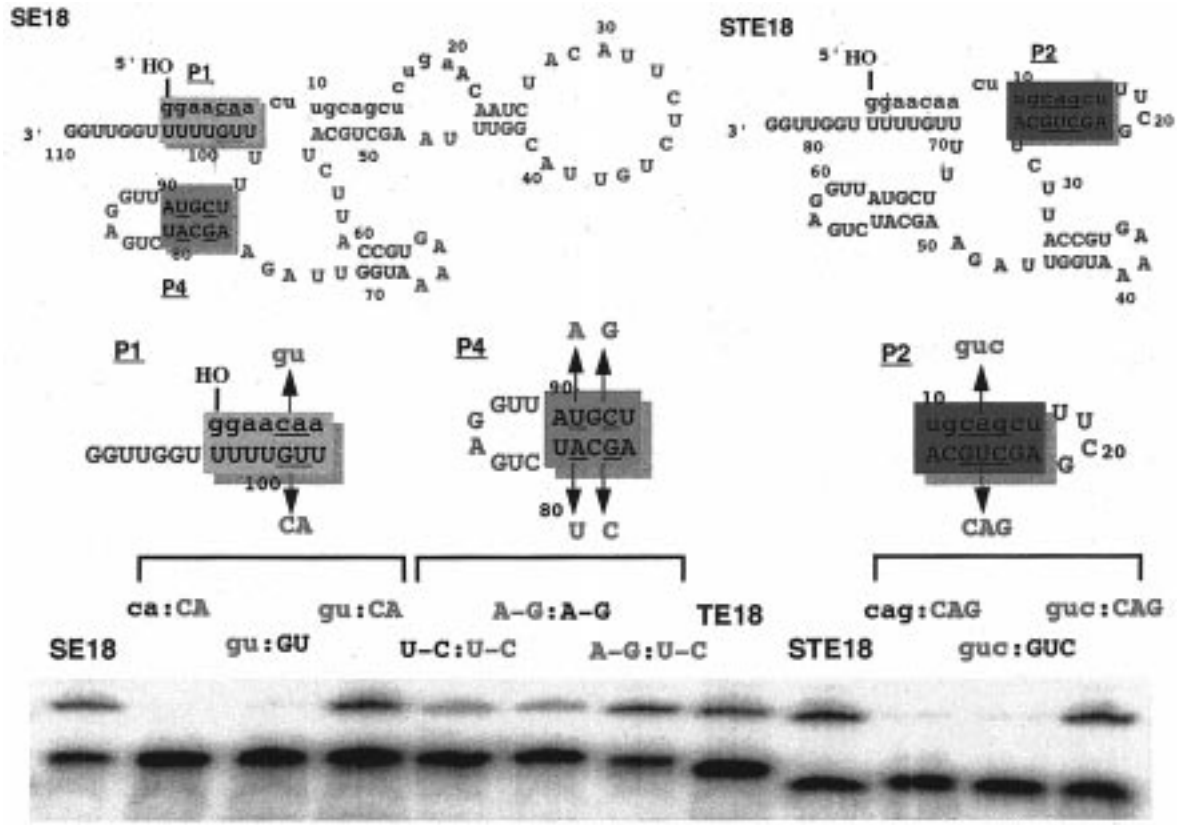

Figure 3. Catalytic activities of mutant ribozymes containing compensatory mutations in stems P1, P2, and P4. Reactions are carried out under saturating substrate conditions ([acyl-donor] = 1 μM) at pH 8.0 and stopped after 1 min of incubation. Abbreviations: Ribz, ribozyme; SAv, streptavidin; Biotin-Met, *N*-biotinylmethionine.

wobble base pair changes were observed (A77:U94 to G77:U94 in clone E15 and C79:G92 to U79:G92 in clone E16). The above data strongly support the existence of stem P3, in which covarying mutations were observed, and are consistent with but do not prove the existence of stems P2 and P4. No evidence concerning paired region P1, the hypothesized pairing between the 5′ region of the ribozyme and the template domain, was obtained because the 5′ region was held constant and the corresponding template domain was invariant.

There is very little sequence conservation in the region between C17 and A47, which may form a relatively unstructured region capping stem P2 (domain 1, pink box in Figure 2B). The relatively high frequency of mutations in this region suggested that it might be unimportant for catalytic activity. To test this possibility, we deleted this region and closed stem P2 with a tetraloop (UUCG), generating a version of clone E18 referred to as TE18 (Figure 2B). The catalytic constants for TE18 are virtually the same as those for E18 (*vide infra*). We have also found that deletion of the 20 nucleotides of the original 3′ constant region (the primer binding site for RT-PCR) from E18 (to generate the shorter clone SE18, see Figure 3) or from TE18 (to generate STE18, see Figure 3) has essentially no effect on catalytic activity.

Because the comparative sequence analysis did not provide solid evidence for the existence of paired regions P1, P2, or P4, mutant ribozymes containing mutations designed to disrupt individual paired regions, and compensatory pairs of mutations designed to restore the paired regions, have been constructed and assayed for activity (Figure 3). Mutants containing mismatched base pairs are virtually inactive (mutations in P1 and P2) or significantly diminished in catalytic activity (mutations in P4). In contrast, the compensatory double mutants in which base pairing is restored retained catalytic activity comparable to that of wild-type ribozyme. These results confirm the secondary structure model illustrated in Figure 2.

Catalytic Activity of Ribozymes. To gain insight into the distinct roles of the template and ribozyme, we have synthesized a small RNA (B27) in which the 5′ (acyl-acceptor) region of the ribozyme is linked directly to the template domain to form a stem-loop (Figure 2B). The direct covalent linkage of the acceptor sequence to the template eliminates the complexities associated with use of a bimolecular acceptor−template complex. This acceptor−template construct should bind the acylated substrate via Watson−Crick base pairing to its complementary sequence on the template and accelerate the acyl-transfer reaction simply by positioning of the acyl group close to the 5′-hydroxyl nucleophile. Comparison of the acceptor−template RNA with the intact ribozyme revealed the rate enhancement due to the nontemplate region of the ribozyme.

Previous studies[18] have indicated that the tandem G:U wobble base pairs in the acceptor−template duplex play an important part in catalysis, probably by acting as the binding site for the catalytic metal ion.[21] We have therefore constructed a mutant ribozyme (WC18, Figure 2B), containing the mutations U102C and U103C so that these consecutive wobble base pairs near the reaction site are replaced with G:C base pairs, and an analogous version of the acceptor−template duplex.

All ribozymes and acceptor−template duplexes obeyed standard Michaelis−Menten-like kinetics for a single turnover reaction with a single saturable substrate binding site. The kinetic behavior observed for the wild-type ribozyme is shown in Figure 4. The rate constants (k_{cat}) and Michaelis constants (K_m) for all ribozymes and acceptor−template duplexes are summarized in Table 1. Deletion of the poorly conserved

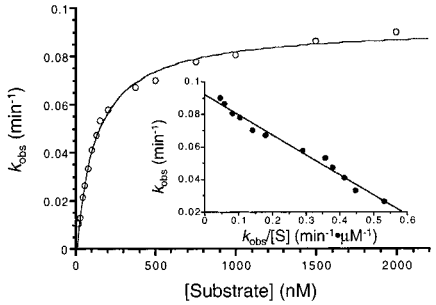

Figure 4. Nonlinear regression curve of Michaelis−Menten-like kinetics (pH 7.0) for acyl transfer reaction catalyzed by E18. The inset graph shows a linear plot according to the Eadie−Hofstee equation.

Table 1. Catalytic Constants of Ribozymes[a]

ribozyme	k_{cat} (min^{-1})	K_m (nM)	k_{cat}/K_m (s^{-1} M^{-1})	rate enhancement
E18	$9.24 \pm 0.13 \times 10^{-2}$	124 ± 6.1	12.4×10^3	2066
TE18	$9.15 \pm 0.11 \times 10^{-2}$	120 ± 9.5	12.7×10^3	2117
SE18	$8.96 \pm 0.15 \times 10^{-2}$	206 ± 6.1	7.25×10^3	1208
STE18	$8.88 \pm 0.17 \times 10^{-2}$	215 ± 8.6	6.88×10^3	1147
WC18	$4.03 \pm 0.12 \times 10^{-3}$	250 ± 8.2	269	45
B27	$2.75 \pm 0.15 \times 10^{-4}$	769 ± 110	6.0	1
WC27	$3.25 \pm 0.21 \times 10^{-4}$	822 ± 150	6.6	1.1

[a] All reactions were carried out at pH 7.0 as described in the Experimental Section.

domain 1 has very little effect on either k_{cat} or K_m. Deletion of the 3′ constant region results in an approximately 2-fold increase in K_m for the acylated substrate, while the k_{cat} values are unchanged. This small increase in K_m is probably due to loss of base-stacking interactions between the 3′ constant region and the adjacent substrate−template duplex. In contrast to the moderate effects of the above deletions, mutation of the tandem G:U wobble base pairs in the template domain to G:C Watson−Crick base pairs decreases k_{cat} by 20-fold (compare WC18 to E18, Table 1).[21] K_m increases only modestly, implying that the G:U wobble base pairs play an important role in catalytic activity but not in substrate binding.

The k_{cat} of the acceptor−template duplex (B27) is approximately 300-fold lower, and the K_m is approximately 3−4-fold larger, than that for the ribozyme. These observations confirm earlier results[18] and indicate that the folded structure of the ribozyme plays an important role in catalysis. The rate enhancement due to the nontemplate part of the ribozyme (domain 2) is about 1000-fold. Close positioning of the 5′-hydroxyl nucleophile and the 3′-acyl group of the substrate by alignment on the template strand contributes greatly to the acceleration of acyl group transfer. In fact, the removal of the internal template sequence completely eliminates detectable catalytic activity of both the ribozyme and the acceptor−template duplex. Therefore, the second-order rate constant for spontaneous acyl-transfer reaction was estimated by extrapolation from the hydrolysis rate ($<10^{-3}$ min^{-1}) under the assay conditions. Assuming that water (55 M) is the nucleophile that accepts the acyl group, the second-order rate constant is 3×10^{-7} s^{-1} M^{-1}. Comparison with the second-order rate constant for the acceptor−template duplex (B27, 6 s^{-1} M^{-1}) leads to a rate enhancement of acyl-transfer due to the template domain of approximately 10^7. The addition of domain 2 to the template domain provides a further rate enhancement of about 10^3, for an overall rate enhancement over the spontaneous acyl-transfer reaction of greater than 10 orders of magnitude.

Mutation of the tandem G:U base pairs to G:C base pairs in the context of the ribozyme leads to a large reduction in k_{cat}, while the same mutations in the acceptor−template duplex alone (WC27) result in a small increase in k_{cat}, showing that the G:U wobble base pairs near the acylation site are effective in increasing catalytic activity only in the context of the ribozyme. Since the tandem G:U wobble base pairs are likely to constitute the binding site of the catalytic metal ion,[21] we have examined the influence of the ribozyme on metal ion binding to this site on the acceptor−template duplex. The apparent K_d for Mg^{2+} (as estimated from the concentration that results in half-maximal rate enhancement) is somewhat weaker for the acceptor−template duplex vs the intact ribozyme and is almost unaffected by the presence of Watson−Crick or wobble base pairs (Table 2). In contrast, $[Co(NH_3)_6]^{3+}$ binds strongly to both the Watson−Crick and wobble acceptor−template duplexes, but binds 3-fold less tightly to the wild-type ribozyme, and 100-fold less tightly to the Watson−Crick mutant ribozyme. The observation that $[Co(NH_3)_6]^{3+}$ (but not Mg^{2+}) binding to the intact ribozyme is weaker than binding to the isolated template domain suggests that the ribozyme may act to distort the metal ion binding site to favor catalysis, in such a way as to result in a loss of $[Co(NH_3)_6]^{3+}$ but not Mg^{2+} affinity; however, we cannot yet rule out the alternative possibilities that there is a change in rate-limiting step with metal ion concentration or between $[Co(NH_3)_6]^{3+}$ and Mg^{2+}.

Table 2. Dissociation and Catalytic Constants of Ribozymes for Mg^{2+} and $Co(NH_3)_6^{3+}$ [a]

	Mg^{2+}		$[Co(NH_3)_6]^{3+}$	
ribozyme	K_d (mM)	k_{cat} (min^{-1})	K_d (mM)	k_{cat} (min^{-1})
E18	14.0	1.32	0.354	1.00
WC18	13.0	0.057	8.5	0.077
B27	22.1	0.0019	0.105	0.0023
WC27	22.2	0.0036	0.088	0.0018

[a] K_d for metal ions and k_{cat} were determined by measuring the initial rate as a function of the concentration of metal ion. Reactions for the full-length ribozymes (E18 and WC18) were carried out under saturating substrate conditions ([acyl-donor] = 1 μM) at pH 8.0 in the presence of 1 mM spermidine. Reactions for the acceptor−template duplexes (B27 and WC27) were also carried out under saturating substrate conditions ([acyl-donor] = 2.5 μM) at pH 8.0 but in the absence of spermidine.[24] The metal ion titration data in all cases fitted a simple single-site saturation curve, and Hill analyses indicated that only one metal ion is required for activity.

Competitive Inhibition by an Unacylated Hexanucleotide. Although the internal template sequence of the ribozyme is essential for catalytic activity, additional interactions between the substrate and the ribozyme could affect substrate binding. The K_m of the ribozyme (STE18, 215 nM) for the acylated substrate oligonucleotide is approximately 3−4-fold smaller than that of the template domain alone (B27, 769 nM), for which Watson−Crick interactions are expected to fully account for substrate binding. This observation initially suggested that additional interactions, perhaps involving the methionyl group, might contribute to substrate binding by the ribozyme. To address this question, we examined the ability of the unacylated hexanucleotide to competitively inhibit the ribozyme. This hexanucleotide inhibitor would compete with the acyl-donor substrate upon binding to the internal template region. If the ribozyme recognizes only the hexanucleotide moiety, the inhibition constant (K_i) for the unacylated hexanucleotide should be comparable to the K_m of the acylated hexanucleotide. On the other hand, if the ribozyme recognizes the amino acid moiety, the K_i should be larger than the K_m.

The catalytic rate constants k_{obsd} for the ribozyme construct STE18 were measured under three different substrate concentrations as a function of the inhibitor concentration (Figure 5).

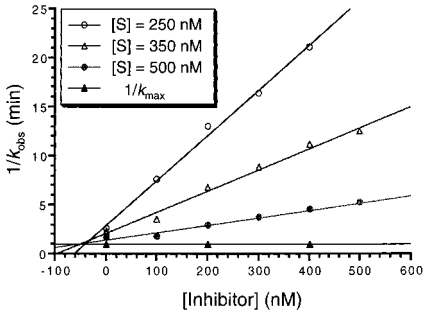

Figure 5. Dixon analysis of STE18-catalyzed acyl transfer reaction in the presence of the unacylated hexanucleotide inhibitor. The reactions were carried out at pH 8.0.

The K_i was estimated to be 40−60 nM, which is approximately 4 times smaller than the K_m. The K_i for the longer ribozyme construct E18 was 20−40 nM (data not shown), which is also approximately 4 times smaller than the K_m. One possible explanation for the apparent smaller value of the K_i values compared to the K_m values is that contamination of the acyl-donor substrate by unacylated hexanucleotide, which could be formed by the hydrolysis, artificially increased the apparent K_m. In fact, we observed that approximately 20% of substrate was hydrolyzed during manipulations after HPLC purification; however, this is clearly insufficient to account for a 4-fold effect.

We propose that the ribozyme interacts with the substrate−template duplex to stabilize substrate binding. The K_m of the template for substrate is approximately 800 nM, and due to the slow rate of the chemical step, this is likely to represent the K_d. Unfortunately it has not been possible to measure a K_i for unacylated oligonucleotide in the template only system, due to the slow rate of the reaction. However, it is unlikely that the acyl group contributes significantly to binding to the template; if we assume that the K_d of the template domain for the unacylated oligonucleotide is also approximately 800 nM, then comparison with the K_i of the ribozyme for the unacylated oligonucleotide (40−60 nM) suggests that the ribozyme stabilizes binding of the oligonucleotide portion of the substrate by 15−20-fold. The higher K_m of the ribozyme for acylated substrate would then be interpreted as due to unfavorable ground-state interactions between the ribozyme and the acyl group. If these unfavorable ground-state interactions are alleviated in the transition state, they may contribute to the overall rate enhancement.

Conclusions

The secondary structure of the acyl-transferase ribozyme has been determined by a combination of sequence comparison and mutant analysis. Knowledge of this secondary structure allowed us to delete nonessential regions of the wild-type sequence, leading to a smaller version of the ribozyme (STE18, 83 nts) that retains essentially full catalytic activity, with only a 2-fold decrease in substrate affinity. This ribozyme is our current starting point in the search for derivatives that are suitable for X-ray crystallographic studies. This ribozyme catalyzes the acyl-transfer reaction 3 orders of magnitude faster than the simple template-directed reaction and approximately 10 orders of magnitude faster than spontaneous, untemplated acyl-transfer reaction. The G:U wobble base pairs near the acylation site play an important role in catalysis, probably by acting in concert with the rest of the ribozyme to form a binding site for the catalytic metal ion. The ribozyme appears to perturb this site so as to increase catalysis, while altering metal ion binding. Kinetic studies indicate that the ribozyme may also stabilize the binding of the substrate oligonucleotide to the template. Contacts with the acyl group may destabilize substrate binding in the ground state, leading to the interesting possibility that one mechanism that contributes to catalysis may be a decrease in these negative interactions in the transition state.

Experimental Section

Synthesis of Acyl-Donor Hexanucleotide. The *N*-biotinylated methionine cyanomethyl ester was prepared by condensation of L-methionine with the *N*-hydroxysuccinimide ester of biotin followed by alkylation of the carboxyl group with chloroacetonitrile.[22] The RNA pCAACCA was prepared manually on CPG (10 μmol scale) using protected ribonucleotide phosphoramidites and a chemical phosphorylation reagent (Glen Research), deprotected in the standard manner, and purified by reversed phase HPLC on a C18 column (Vydac) with a linear gradient (1 mL/min, 0−80% acetonitrile in 0.1 M triethylammonium acetate, pH 4.5 over 20 min). Lyophilized pCAACCA-triethylammonium salt (0.5 μmol) was dissolved in 5 μL of aqueous 0.5 M tetrabutylammonium hydroxide (TBAOH), and 5 μL of 0.5 M *N*-biotinylated methionine cyanomethyl ester in DMF was quickly added. After 1 h of stirring at room temperature, another 5 μL each of the TBAOH and cyanomethyl ester solution were added, and the mixture was stirred for an additional 1.5 h. The reaction was quenched by adding 0.5 μL of AcOH, and the acylated hexamer was purified by reversed phase HPLC on a C18 column under the same conditions described above. The purified product was concentrated by a speed vacuum system, and the pellet was dissolved in water.

Ribozyme Synthesis. Ribozymes were synthesized by T7 RNA polymerase runoff transcription of PCR DNA templates in the presence of α-^{32}P UTP. The transcripts were treated with RNase-free DNase (Promega) for 30 min. Products were purified by denaturing polyacrylamide gel electrophoresis and were eluted from the gel in 0.3 M NaCl. The ethanol-precipitated RNA was dephosphorylated by treatment with calf intestinal phosphatase (New England BioLab) for 1 h, and the product was isolated by phenol−chloroform extraction followed by ethanol precipitation.

General Kinetics. Reactions were carried out as follows: A total of 48 μL of a ribozyme solution was prepared by mixing of 6 μL of 300 nM ribozyme (10×) with 15 μL of 4× buffer (400 mM KCl, 100 mM HEPES, pH 7.0) and 27 μL of water, heating at 90 °C for 5 min, and sitting at 25 °C for 5 min. To this solution was added 6 μL of 0.5 M $MgCl_2$, and the mixture was incubated for 5 min. Reactions were initiated by the addition of 6 μL of various concentration of acyl-donor hexanucleotide substrate to the ribozyme solution and incubated for various times. Reactions were stopped by taking 6 μL of the reaction mixture into 3 μL of quenching buffer containing 8 M urea, 70 mM EDTA, 42 μM streptavidin,[23] and 50 mM Tris·HCl adjusted at pH 6.0. Samples were subjected to electrophoresis on 6% polyacrylamide, 8 M urea gels running in a cold room to keep the gel temperature below 30 °C. Velocities were determined by taking at least 5 points from the linear regions of the time course. The yield of 5′-acylated ribozyme (X = OH) reached a plateau at approximately 50% after 20 min, suggesting that only half of ribozyme was active probably due to the incorrect folding of the sequence. Catalytic constants were corrected to reflect 50% functional ribozyme concentration.[18]

Synthesis of Mutant Ribozymes and Assays for Catalytic Activity. The DNA template of E18[18] was amplified by PCR in the presence of appropriate primers to introduce the mutations. The PCR was carried out 20 cycles to ensure that the amplified DNA contains less than 0.001% of the original DNA template. Ribozymes were synthesized

(22) Robertson, S. A.; Ellman, J. A.; Schultz, P. G. *J. Am. Chem. Soc.* **1991**, *113*, 2722−2729.

(23) Ulanovsky, L.; Drouin, G.; Gilbert, W. *Nature* **1990**, *343*, 190−192.

(24) The catalytic activity of the template ribozymes were strongly inhibited by the addition of 1 mM of spermidine. Since the structure of the template ribozymes is a simple stem-loop, the titratable metal ion concentration for these ribozymes should be the catalytic metal ion rather than structural one.

by T7 RNA polymerase runoff transcription of PCR DNA templates, as described above. Assays for catalytic activity were carried out as described above, except for the use of 6 μL of 10 μM substrate, giving 1 μM at the final concentration. Under these conditions, all ribozymes are saturated with the substrate so that the observed rate constant (k_{obsd}) for each ribozyme should approximate its maximal value (k_{cat}).

Inhibition by Hexanucleotide. Reactions were carried out as follows: A total of 42 μL of a ribozyme solution was prepared by mixing of 6 μL of 300 nM ribozyme (10×) with 15 μL of 4× buffer (400 mM KCl, 100 mM HEPES, pH 8.0) and 27 μL of water, heating at 90 °C for 5 min, and sitting at 25 °C for 5 min. To this solution was added 6 μL of 0.5 M $MgCl_2$, and the mixture was incubated for 5 min. Reactions were initiated by the addition of a total of 12 μL of mixture of acyl-donor substrate and hexanucleotide inhibitor to the ribozyme solution and incubated for various times. The concentrations of substrate and inhibitor were adjusted as shown in Figure 5. The remaining procedures were carried out as described above.

Metal Titration Experiments. A total of 42 μL of a ribozyme solution was prepared by mixing 6 μL of 300 nM ribozyme (10×) with 15 μL of 4× buffer (400 mM KCl, 100 mM HEPES, pH 8.0) and 27 μL of water, heating at 90 °C for 5 min, and cooling to 25 °C for 5 min. To this solution was added 6 μL of 10 mM spermidine (or 6 μL of water for B27 and WC27) and 6 μL of divalent metal ion solution with various concentrations, and the mixture was incubated for 5 min. Reactions were initiated by the addition of 6 μL of 10 μM substrate to the ribozyme solution (or 25 μM substrate for B27 and WC27) and incubated for various times. The remaining procedures were performed as described above.

Acknowledgment. We thank Drs. David Huizenga and David Wilson for helpful discussions. This work was supported by NIH grant R01 GM53936 to J.W.S.

JA972472S